GALILEO GALILEI (GG)

CONSOLIDATED MISSION DESCRIPTION DOCUMENT

DRL/DRD: DEL-29

Written by	Responsibility
G. B. Amata	Author
Verified by	
A. Anselmi	Checker
Approved by	
	Product Assurance
	Configuration Control
	Design Engineer
	System Engineering Manager
A. Anselmi	Study Manager
Documentation Manager	
R. Cavaglià	

The validations evidence are kept through the documentation management system.

CHANGE RECORDS

ISSUE	DATE	§ CHANGE RECORDS	AUTHOR
01	08-Jun-09	First issue submitted to PRR Versions of parts of this report were circulated previously under SD-TN-AI-1168 “GG Mission Analysis Report”	

TABLE OF CONTENTS

LIST OF FIGURES

LIST OF TABLES

1. INTRODUCTION

This document is submitted in partial fulfilment of Work Package 1A-ADA of the GG Phase A2 Study (DRL item DEL-29).

The purpose of this document is to provide the reference GG mission design, and the justification thereof, for the purposes of the GG Phase A2 study.

It will be maintained as an applicable document in the future phases of the project.

CONTROLLED DISTRIBUTION

2. REFERENCES

2.1 Applicable Documents

[AD 1] ASI, "Progetto Galileo Galilei-GG Fase A-2, Capitolato Tecnico", DC-IPC-2007-082, Rev. B, 10-10-2007 and applicable documents defined therein

2.2 Standards

[SD 1] ECSS-M-00-02A, Space Project Management – Tailoring of Space Standards, 25 April 2000

[SD 2] ECSS-E-ST-10C, Space Engineering - System Engineering General Requirements, 6 March 2009

[SD 3] ECSS-E-10-02A, Space Engineering – Verification

[SD 4] ECSS-Q-00A, Space Product Assurance - Policy and Principles, and related Level 2 standards.

2.3 ASI Reference Documents

[RD 1] GG Phase A Study Report, Nov. 1998, revised Jan. 2000, available at: http://eotvos.dm.unipi.it/nobili/ggweb/phaseA/index.html

[RD 2] Supplement to GG Phase A Study (GG in sun-synchronous Orbit) "Galileo Galilei-GG": design, requirements, error budget and significance of the ground prototype", A.M. Nobili et al., Physics Letters A 318 (2003) 172–183, available at: http://eotvos.dm.unipi.it/nobili/documents/generalpapers/GG_PLA2003.pdf

[RD 3] A. Nobili, DEL001: GG Science Requirements, Pisa, September 2008

2.4 GG Phase A2 Study Notes

[RD 4] SD-RP-AI-0625, GG Final Report / Satellite Detailed Architecture Report, Issue 1

[RD 5] SD-RP-AI-0626, GG Phase A2 Study Executive Summary, Issue 1

[RD 6] SD-TN-AI-1163, GG Experiment Concept and Requirements Document, Issue 3

[RD 7] SD-RP-AI-0620, GG System Performance Report, Issue 2

[RD 8] SD-TN-AI-1167, GG Mission Requirements Document, Issue 2

[RD 9] SD-RP-AI-0590, GG System Concept Report (Mission Description Document), Issue 3

[RD 10] SD-SY-AI-0014, GG System Functional Specification and Preliminary System Technical Specification, Issue 1

[RD 11] SD-RP-AI-0631, GG Consolidated Mission Description Document, Issue 1

[RD 12] SD-TN-AI-1168, GG Mission Analysis Report, Issue 2

[RD 13] DTM, GG Structure Design and Analysis Report, Issue 1

[RD 14] SD-RP-AI-0627, GG Thermal Design and Analysis Report, Issue 1

[RD 15] SD-RP-AI-0268, GG System Budgets Report, Issue 1

[RD 16] SD-RP-AI-0621, Technical Report on Drag and Attitude Control, Issue 2

[RD 17] TL25033, Payload Architectures and Trade-Off Report, Issue 3

[RD 18] SD-RP-AI-0629, Technical Report on Simulators, Issue 1

[RD 19] GG.ALT.TN.2003, FEEP Microthruster System Technical Report, Issue 1

[RD 20] TASI-FI-44/09, Cold Gas Micro Thruster System for Galileo Galilei (GG) Spacecraft - Technical Report, Issue 1, May 2009

[RD 21] SD-RP-AI-0630, Spin Sensor Design, Development and Test Report, Issue 1

[RD 22] SD-TN-AI-1169, GG Launcher Identification and Compatibility Analysis Report, Issue 1

[RD 23] ALTEC-AD-001, GG Ground Segment Architecture and Design Report, Issue 1

[RD 24] SD-TN-AI-1218, GG Preliminary Product Tree, Issue 1

[RD 25] SD-PL-AI-0227, GG System Engineering Plan (SEP), Issue 2

[RD 26] TAS-I, Payload Development and Verification Plan, Issue 1

[RD 27] SD-PL-AI-0228, GG System Verification and Validation Plan, Issue 1

[RD 28] SD-TN-AI-1219, Report on Frequency Management Issues, Issue 1

[RD 29] SD-RP-AI-0632, GG Mission Risk Assessment And Mitigation Strategies Report, Issue 1

[RD 30] SD-RP-AI-0633, Report on Mission Costs Estimates, Issue 1

2.5 External Reference Documents

[RD 31] Arianespace, VEGA User's Manual, Issue 3, Revision 0, March 2006

[RD 32] Future Solar Activity Estimates for Use in Prediction of Space Environmental Effects on Spacecraft, NASA-MSFC Monthly Report, June 2008.

3. REFERENCE MISSION PROFILE

3.1 General Description

The GG mission is devoted to a single experiment that, once initialized, runs to the end of the scientific data collection. After the launch and early orbit phase, experiment set-up and first calibration operations are executed. Thereafter, the experiment is run in 7-day long data collection intervals. Calibration sessions are regularly interspersed with the measurement intervals. Continuation of the mission improves the measurement accuracy with the square root of the measurement time. The nominal duration of the mission is two years.

No orbital change manoeuvres are required after acquisition of the operational orbit, approximately 1.5 hours after lift-off. The processing of scientific data is done in bulk; therefore no scientific quick-look is required. All scientific operations are autonomous, executed on the basis of time-tagged operation sequences that are loaded at least one day in advance. Given the high level of autonomy, the tasks of the ground control are essentially limited to:

- Commanding and monitoring of the attitude manoeuvres (initial spin axis orientation and spin-up)
- Generation and transmission of command sequences and parameters
- Analysis of satellite data to establish that the satellite is operating correctly.

The mission is performed in equatorial circular orbit. The dedicated ground station is San Marco, Malindi, Kenya. The ground passes occur according to the sequence described in Section 4. Support by other stations in the early orbit phase may be considered.

As it is customary, the ground segment will include, besides the ground station, an Operational Control Centre (OCC), responsible of the execution of the mission operations, and an Operational Scientific Centre (OSC), responsible of the generation of the scientific operation sequences. There is no special requirement for real-time interaction between the on-board payload and the OSC, or, in general, between the satellite and the OCC.

A generic timeline of the mission is provided in Table 3.1-1.

Launch and Ascent Phase	
duration: ≈1 hour	3-axis stabilized release by the launcher satellite off on lift-off; activation of OBDH and RF by separation switch
Early Orbit Phase	
duration: ≈1 day	sun acquisition, rate damping and coarse spin attitude stabilization (autonomous) satellite acquisition by the EOP ground station network satellite health check
Satellite Commissioning	
duration: ≈1 week	satellite control handed over to the dedicated ground station subsystem commissioning satellite spin-up (semi-autonomous, assisted by the ground station)
Payload Switch-on and Calibration	
duration: ≈3 weeks	FEEP thruster switch on (pre-calculated thrust profile) Coarse thruster calibration Activation of electrostatic dampers common-mode sensing PGB unlocking Activation of common-mode sensing Activation of drag-free control Activation of spin rate control Test mass unlocking Test mass centering & alignment Fine test mass set-up / iteration
Scientific Mission	
duration: 1 years	Routine data collection Calibration
Scientific Mission Extension (optional)	
duration: until consumables are exhausted	Same sequence as in the Scientific Mission

Table 3.1-1: Sequence of events

3.2 Launch and Early Orbit Phase

The satellite will be launched directly into near-circular, near-equatorial orbit by a small / medium launcher such as Vega (baseline) or PSLV (backup). Both launchers have capability much in excess of a small spacecraft such as GG, and a dual launch might be taken into consideration. Figure 3.2-1 shows the capability of the Vega launcher [RD 31].

The design launch altitude will be between 500 km and 700 km, according to the strategy discussed below (Chapter 5). No orbit maintenance is planned, and the spacecraft altitude will be allowed to decay gently in time, with negligible impact on the satellite mission and operations.

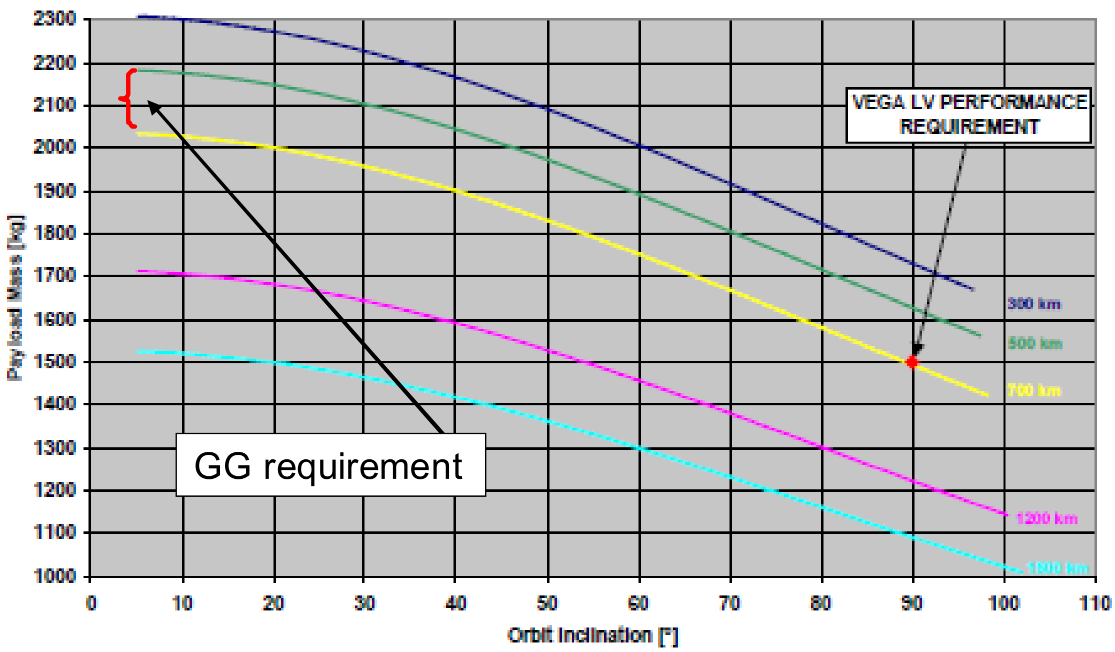

Figure 3.2-1: VEGA performance for circular orbits.

The VEGA launcher design requirement is 1500 kg in a 700-km altitude polar orbit. The lower limit to the orbit inclination is about 5°, and is set by the latitude of the Kourou launch site (5.25°N). For such a near-equatorial orbit, as required by GG, the VEGA performance is in excess of 2000 kg, much above the needed spacecraft mass.

3.3 Experiment Initialization, Calibration and Control

After commissioning at the beginning of life, the main operational modes of the satellite are:

a) Experiment Set-up and Calibration Mode
b) Normal mode (scientific operation of the experiment)
c) High-rate Data Collection Mode
d) Safe (Hold) Mode.

The experiment set-up phase will be based on semi-autonomous procedures, possibly with intermediate checks by the ground after each phase before the next operation is executed. The experiment set-up includes the balancing of the test masses and the mechanical balancing of the capacitance read-out sensors. Both operations need to be repeated at regular intervals. Automatic procedures for such operations will be elaborated, possibly with some interaction with the ground control.

In the science measurements phase, the operation will be essentially autonomous. The Normal Mode is characterized by the drag-free control, executed by proportional microthrusters. However, the survival of the mission does not depend on the drag-free control, since the maintenance of the operational attitude is guaranteed by the gyroscopic stability. In case of malfunctions, the scientific operations will be put on hold and housekeeping data will be collected and transmitted to ground on the next station passes; resumption of the operations will be commanded by the ground.

Generally, the command and parameter sequences of the Normal mode will need to be updated on a time basis of several weeks, except in the set-up phase when the frequency will be higher (some hours).

The scientific data are sent to ground after demodulation, and the telemetry rate is generally small. Exceptionally, it may be necessary to transmit to Earth the raw (non demodulated) data, for special checkout, parameter identification, and troubleshooting. Because of the nature of the experiment, it is anticipated that the duration of such high rate data collection periods does not need to be longer than about 10 minutes. Therefore, the telemetry capacity of the telecommunication links is not exceeded.

3.4 Nominal Mission

The scientific data comprise the position of the test masses relative to each other and the “laboratory” (PGB), the time, the spin reference signal and ancillary data such as the temperature, the attitude of the spin axis and the phase difference between the PGB and the spacecraft’s outer vessel (see Table 3.4-1).

The scientific data collection rate is small, about 20 kbit/s, and the total telemetry rate is well below the limit data rate (1 Mbps) of the ESA S-band ground stations, including Malindi, even in the worst case of 12-hour autonomy from the ground. In normal circumstances, we assume the data are downloaded to ground once every four station passes [RD 4].

The data set needed for post-processing and elaboration of the scientific products include the data in Table 3.4-1 above plus the spacecraft positional data. Tracking with a normal accuracy of several km along-track is sufficient for the purposes of the scientific mission.

The minimum integration time of the experiment is determined by the thermal noise and is about 7 days. Hence, examination of the scientific data at shorter intervals is, strictly speaking, not significant. Therefore, quick look procedures are not needed and the scientific data can be routed to the Scientific Data Centre within a couple of days of reception.

On the other hand, for the purposes of checking the health of the scientific payload and the correct execution of the measurement procedures, shorter reaction times may be desirable. Tests based on consistency checks, threshold parameter values etc. will be elaborated and implemented in automatic self-check procedures that can be run periodically by the onboard computer, and can be used to alert the ground control of any non-nominal state of the scientific payload. Data affected by anomalies of any sort will be rejected on post-processing and will have no effect but a shortening of the data collection period.

The tasks of the Operational Control Centre (OCC) will comprise, besides the normal spacecraft operations (mission planning, monitoring and control; orbit and attitude determination), also the execution of the operations required by the scientific measurements. The OCC will be responsible for routing of the payload telemetry to the Operational Scientific Centre (OSC), and processing of the telecommand requests from the OSC. Co-location of experimenter staff at the OCC, particularly during the early set-up phase, when interaction with the payload on board is more frequent, may be considered.

The data set resulting from the mission will be archived on CDROM and put at the disposal of the scientific community. The complete data set will include raw data, calibrated data and support data (housekeeping, tracking and attitude). The complete data set is expected to comprise about 26 Gbit.

CONTROLLED DISTRIBUTION

Data description	Variable list	Number of variables	Freq. [Hz]	Record length [bit]	Data rate [kbit/s]
Diff. TMs displacement	Δx, Δy	2	50	16	1.6
Tme/PGB displacement	Δx, Δy, Δz	3	50	16	2.4
Tmi/PGB displacement	Δx, Δy, Δz	3	50	16	2.4
PGB/Spacecraft displac.	Δx, Δy, Δz	3	50	16	2.4
ω_{SPIN}	ω_x, ω_y, ω_z	3	50	16	2.4
Reference time	t	1	50	16	0.8
Science data					**12.0**
PGB whirl monitoring	Sensing + actuation	6	1	16	0.096
Tme whirl monitoring	Sensing + actuation	6	1	16	0.096
Tmi whirl monitoring	Sensing + actuation	6	1	16	0.096
ADC monitoring	Number of ADC	9	1	16	0.144
Inchworm monitoring	Number of inchworms	6	1	16	0.096
Piezo monitoring	Number of piezo	6	1	16	0.096
PGB Inner temperature monitoring	Number of temperature sensors	20	0.10	16	0.03
Capacitance bridge monitoring	Number of capacitance bridges	9	0.10	16	0.01
Payload HK					**0.7**
Commands to FEEP	Number of commands	6	1	16	0.096
PGB/Spacecraft phase lag	Number of lag sensors	1	0.10	16	0.0016
Commands to actuators	Number of commands	6	50	16	4.8
Sun sensor	1 (2 in case o redundancy)	2	50	16	1.6
FEEP monitoring	Number of FEEP	6	1	16	0.096
DFACS					**6.6**

Table 3.4-1: Science and Ancillary Data Types

3.5 Extended Mission

The nominal life of the mission in 1 year after the end of the commissioning phase. In this time span, on the order of 50 measurement cycles will be performed. The factors limiting the life of the experiment include:

- The amount of Caesium in the propellant reservoirs of the FEEP thrusters. The current specification is 4500Ns total impulse [RD 15], sufficient for 2 years under worst-case drag environment assumptions.
- The drift of the spin axis in case of loss of 1 thruster [RD 16]. The main effect is a decreasing magnitude of the signal in the detection plane, and several years of continuing measurements are likely to be possible even under spin axis drift.

Eventually, the mission will be terminated by orbit decay, the time scale of which is more than 10 years if the mission is launched after 2014 (see §4.3).

4. ORBIT CHARACTERISTICS AND EVOLUTION

4.1 Eclipse

The eclipse times are important for the preliminary sizing of the s/c, in particular for what concerns the power subsystem. For this analysis an orbit at 520 km altitude was assumed. Figure 4.1-1 below shows the trend of the eclipse durations on a time span of three years (form 2015 to 2018); these durations are considered as the sum of the umbra and penumbra phases, since the model considered is the conical one. The results here represented have been obtained with an STK analysis.

The mean eclipse duration is 35.2 minutes.

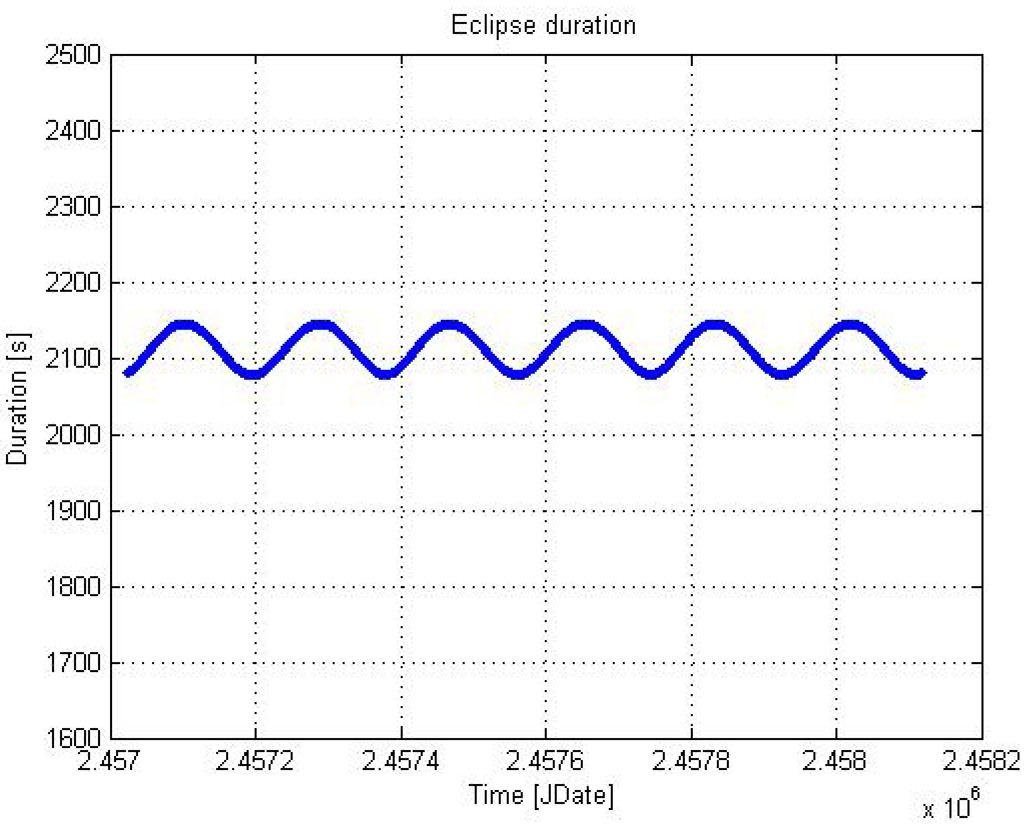

Figure 4.1-1: Eclipse duration in 520 km orbit

4.2 Ground Station Coverage

The ground station considered for the contacts analysis is Malindi. Its position and characteristics are reported in Table 4.2-1.

The simulation was run for one day. As shown in Figure 4.2-1 below, 14 contacts per day occur between the ground station and the s/c. The contact duration is about 10 minutes (mean value 597.6 s).

Ground Antenna Location, Diameter	Latitude [deg]	East Longitude [deg]	Altitude [m]	Usage in GG
Kourou, 15 m	5.25°	-52.80°	-14.7	LEOP
Malindi, 10 m	-2.996°	40.196°	-12.75	LEOP Nominal Mission

Table 4.2-1: Ground Station Characteristics

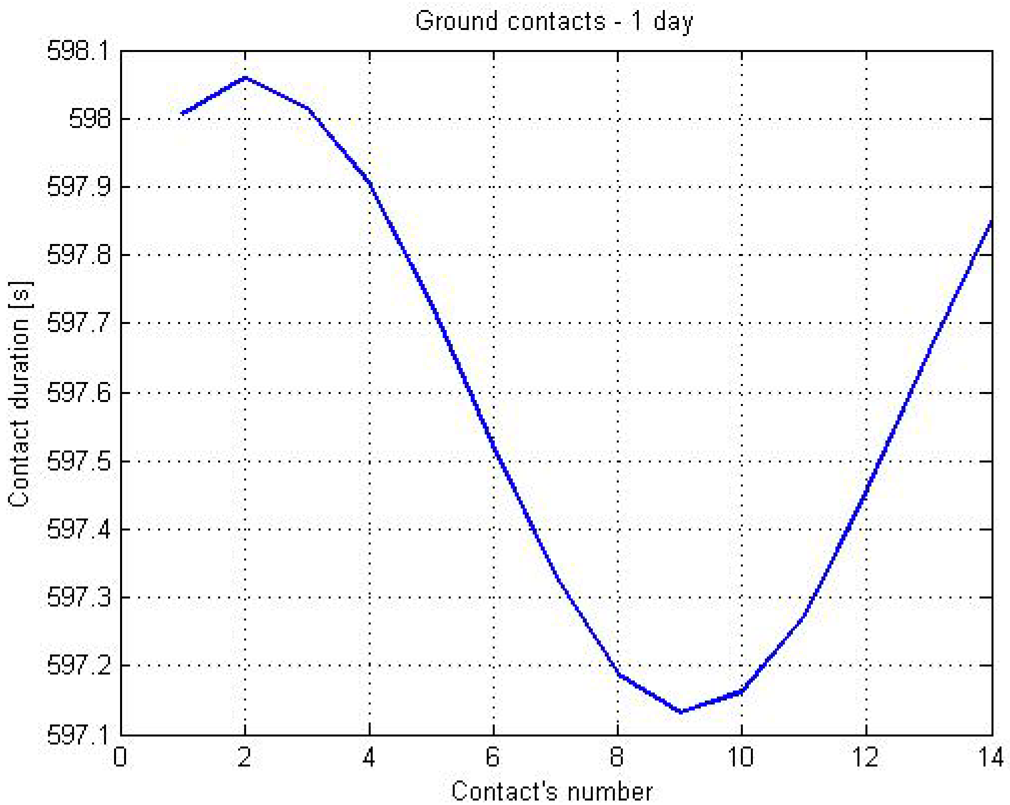

Figure 4.2-1: Contacts duration for 520 km orbit

4.3 Orbit Decay

Atmospheric drag will cause a secular decay of the semi-major axis of the GG orbit, eventually leading to re-entry. The semi-major axis drop will have an effect on the eclipse pattern and the ground contact times. However, for the first years of the mission (1 year nominal life + 2 years extended life) these effects are minor and they can be neglected, as shown below.

The semi-major axis drop was calculated with an in-house orbit analysis tool (Orbitool) using the MSIS-90 density model and the NASA 95% prediction for the solar flux index F10.7 (see chapter 5.2). The initial altitude was 520 km and the calculation was carried out for 1 year at epochs 2013 (worst solar activity condition), 2015 and 2019 (minimum solar flux activity). The area-to-mass ratio was 0.0046 m²/kg.

The next figures show the evolution of the mean altitude over a spherical earth (mean semi-major axis minus mean Earth radius). The effect of the launch date on the predicted decay is evident.

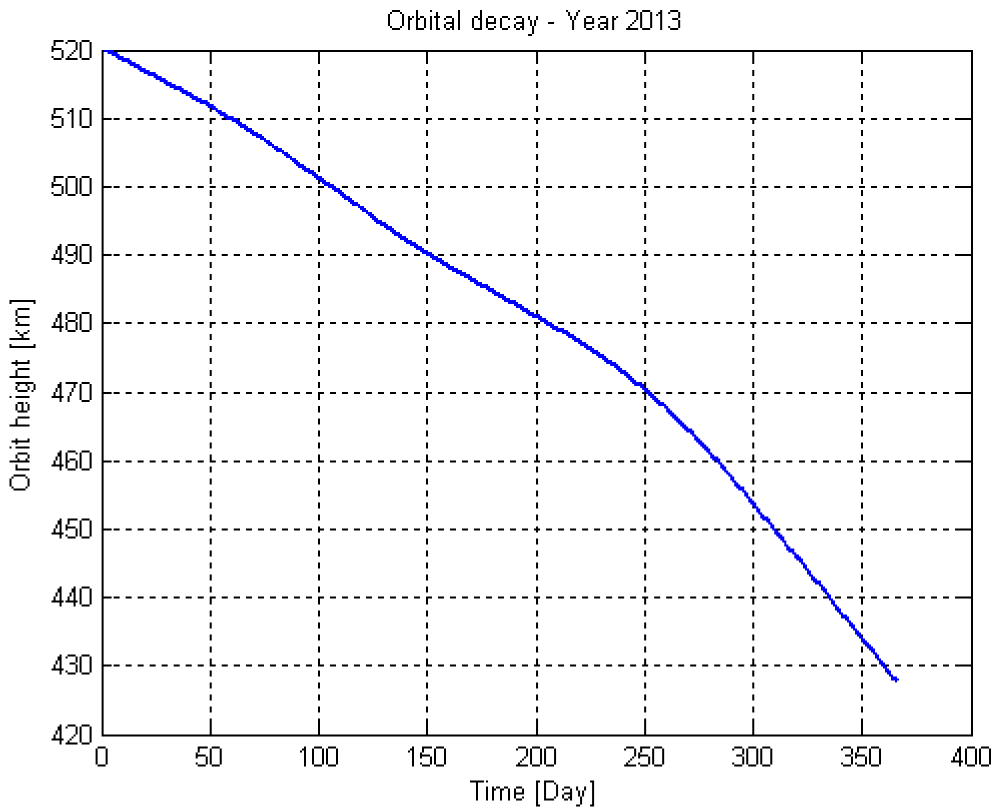

Figure 4.3-1: Orbital decay 520 km – Year 2013

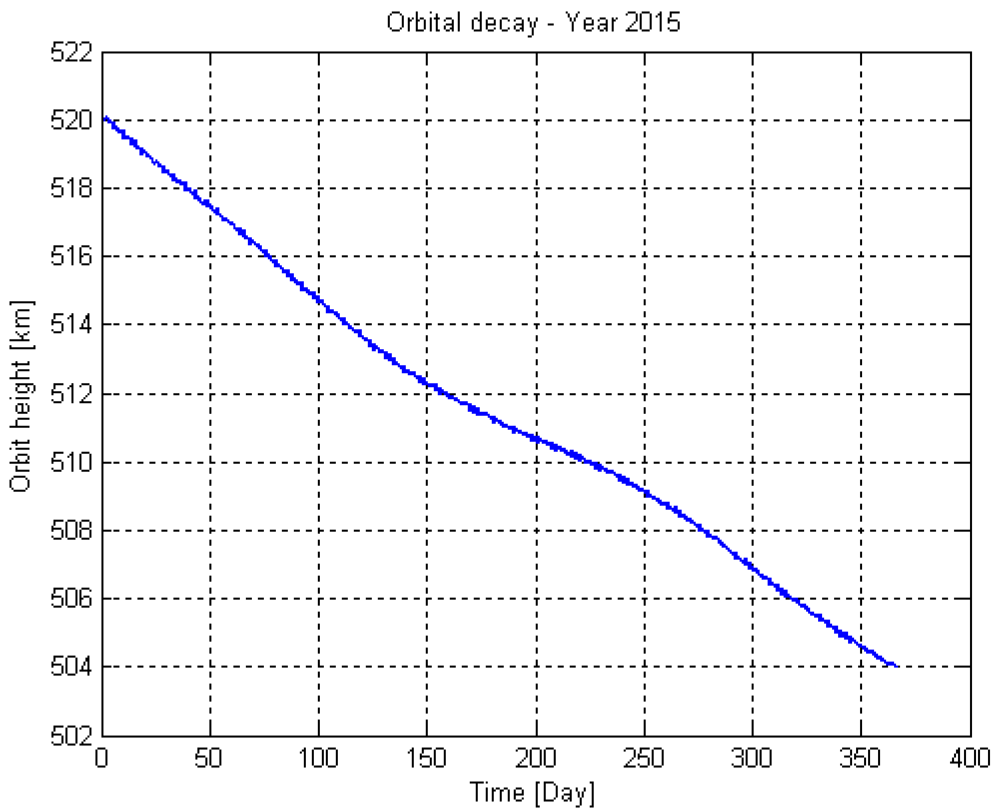

Figure 4.3-2: Orbital decay 520 km – Year 2015

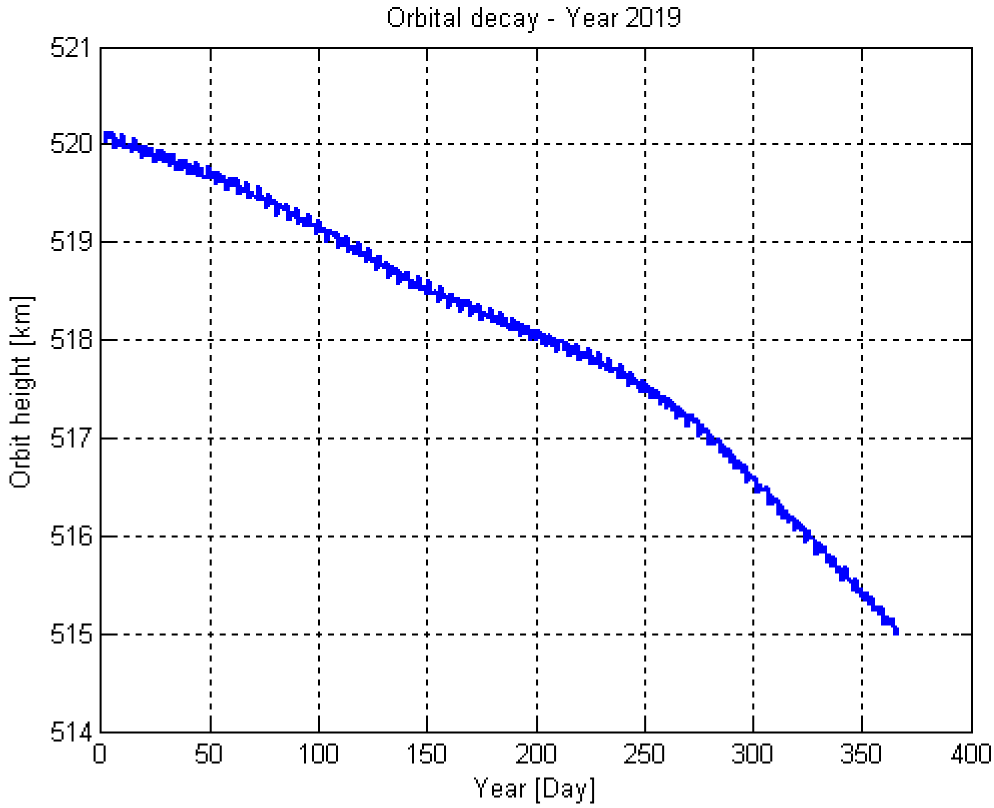

Figure 4.3-3: Orbital decay 520 km – Year 2019

5. ORBIT PERTURBATIONS ANALYSIS

5.1 Spacecraft Geometric Model

To perform the disturbance computation analysis, a simplified configuration for the s/c has been considered. It has been modelled as described in Table 5.1-1 and Figure 5.1-1.

The separated satellite mass has been considered equal to 450 kg.

Property	Units	Value
Cylinder radius	mm	725
Cylinder height	mm	1420
Specular reflection coeff.	-	0.15
Drag coefficient	-	2

Table 5.1-1: Satellite properties

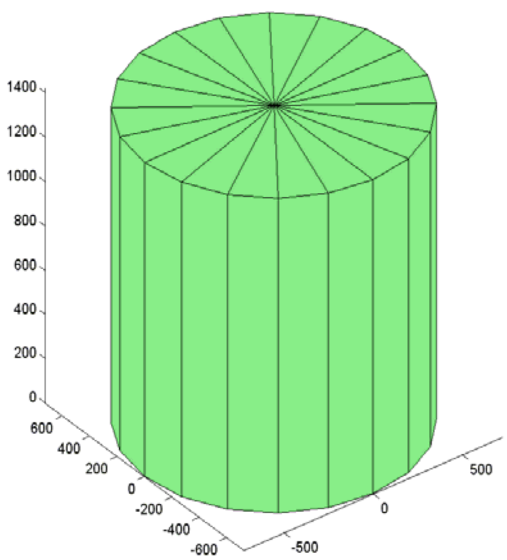

Figure 5.1-1: GG simplified geometry [mm]

The forces are computed in the LORF (Local Orbital Reference Frame) reference frame. The satellite's X axis is directed as the velocity vector while the Y axis is directed as the orbit normal. Finally the choice of a right handed reference frame, defines the satellite's Z axis (Figure 5.1-2).

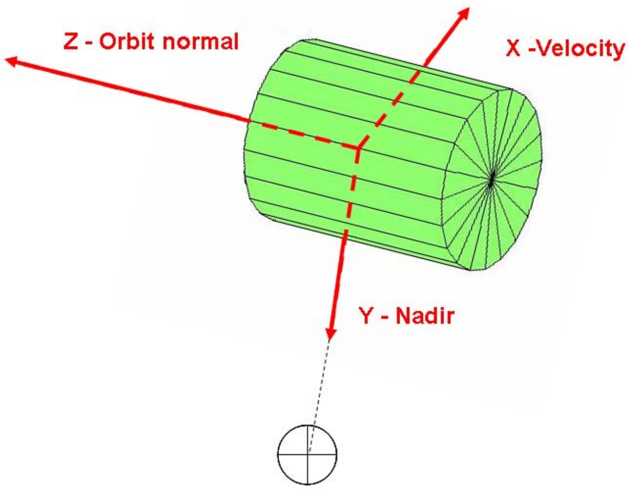

Figure 5.1-2: Definition of the local orbital reference frame

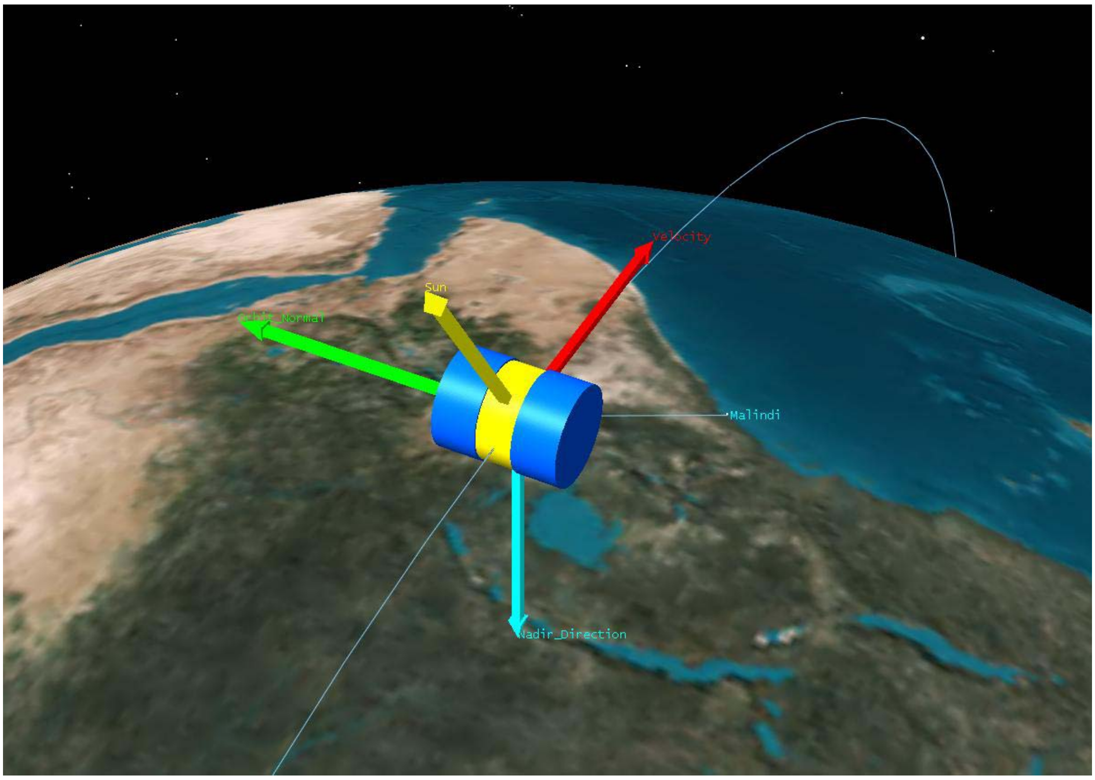

Figure 5.1-3: S/c orbit

5.2 Perturbation Model

A parametric study of the air drag was performed for circular orbits in the altitude range between 520 km and 800 km, in the years from 2013 to 2020.

The density values are provided by the MSIS-E-90 model and are highly dependent on the values of solar activity. The scale height of Earth's upper atmosphere (and thus the drag on satellites in low Earth orbit) is dependent on the intensity of short-wavelength solar radiation and the level of geomagnetic activity, so knowledge of the profile and magnitude of the next solar and geomagnetic cycles is crucial for accurate mission simulations. The most relevant indexes that define solar and geomagnetic activity are: F10.7 (solar radio noise flux at a wavelength of 10.7 cm) and Ap (daily global index of geomagnetic activity). The predicted values for F10.7 for the MSAFE Model are shown in next figure for the time period [2007, 2023] and for various confidence levels. For solar activity predictions in the perturbations analyses, the maximum values (95% confidence level) of the MSAFE Model have been used as the worst-case scenario.

In the time interval considered, 2013 is the worst case and the predicted flux decreases until the next minimum in 2019.

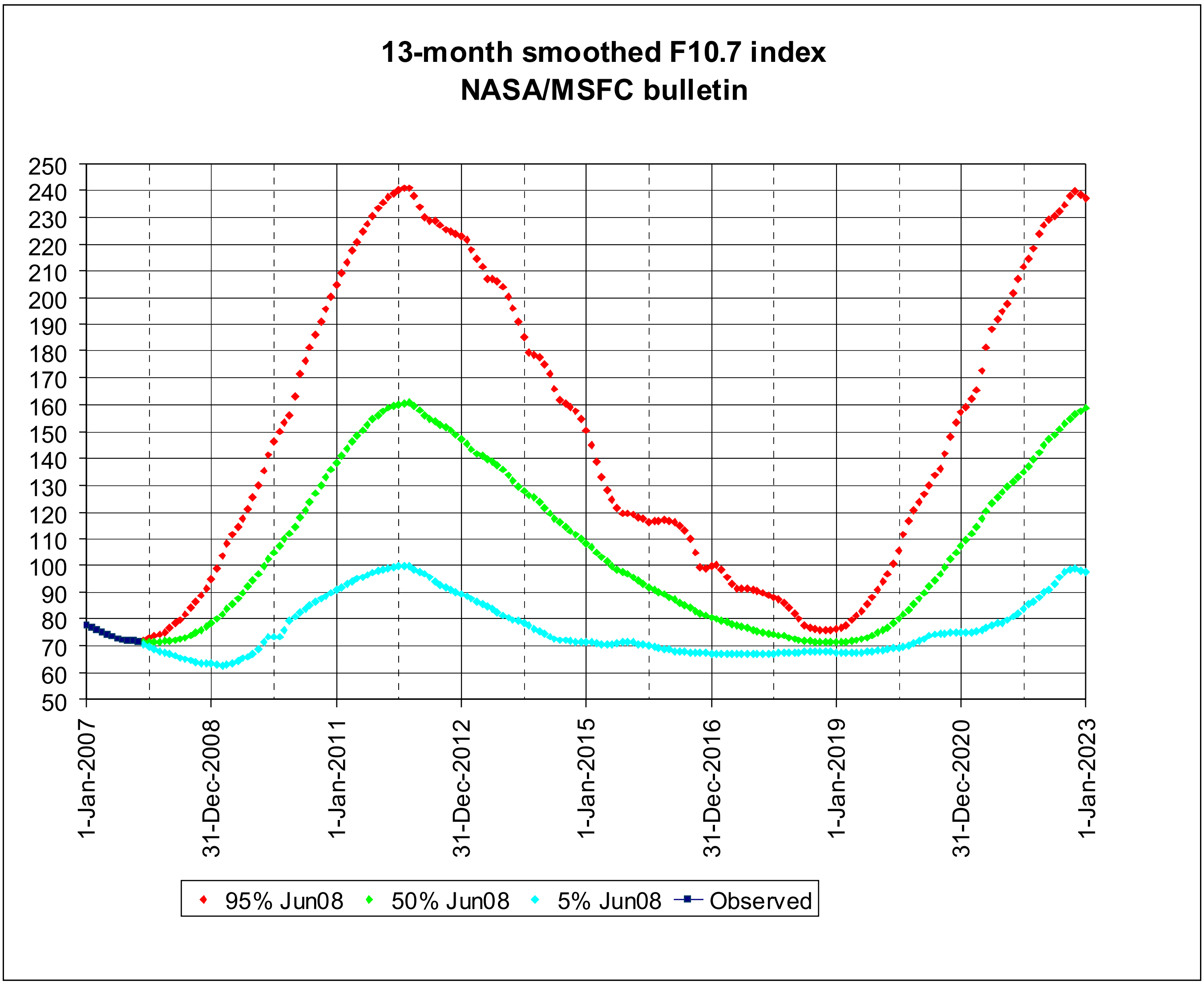

Figure 5.2-1: NASA forecast of F10.7 parameter [June 2008 bulletin]

5.3 Air Drag Force Parametric Analysis

The study addressed nominally circular, equatorial orbits at mean altitudes between 520 km and 800 km.

To perform a drag force analysis, the geometry and perturbation models previously described were assumed. The MSAFE Model was used with the confidence level of solar flux prediction equal to 95%.

Figure 5.3-1 to Figure 5.3-8 show the components of the drag force and acceleration in one day period at 520 km and 800 km and in two years corresponding respectively to the mean and minimum of solar activity (the used system reference frame is the one presented in paragraph 5.1).

Figure 5.3-9 shows the parametric analysis of the maximum acceleration per orbit, as function of epoch, for a number of altitudes. The maximum forces value previously calculated at different orbit altitudes and epochs were divided by the s/c mass of 450 kg to obtain the accelerations. The maximum acceleration threshold level is of 2×10^{-7} m/s^2.

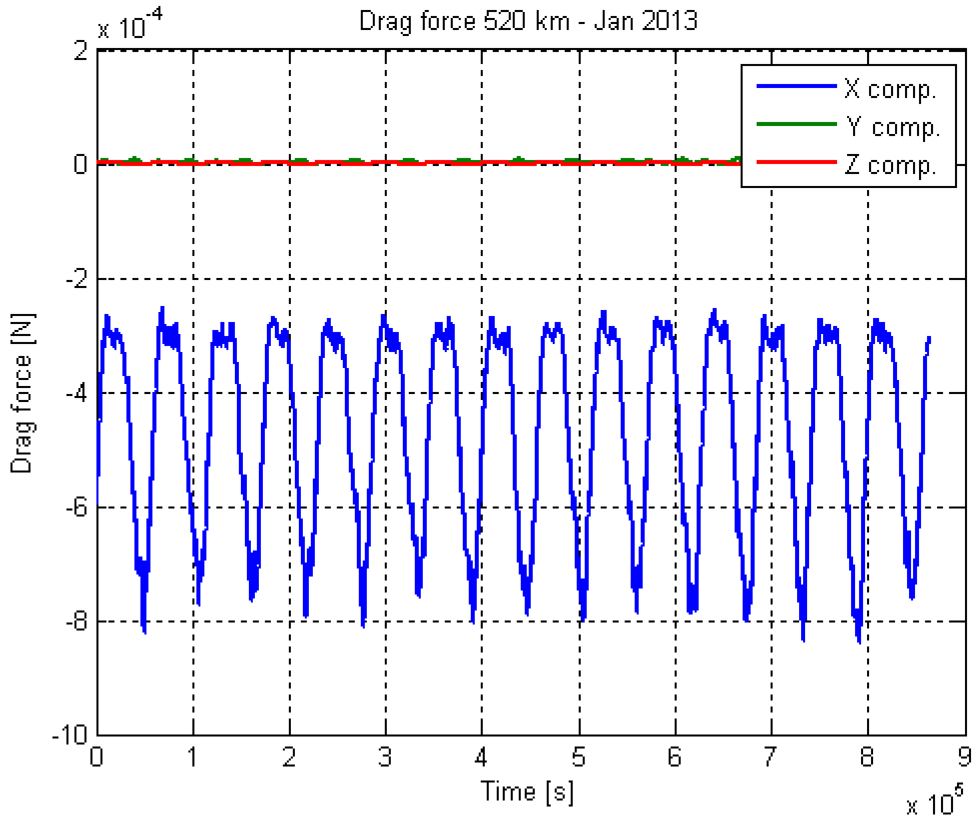

Figure 5.3-1: Drag force at 520 km - Year 2013

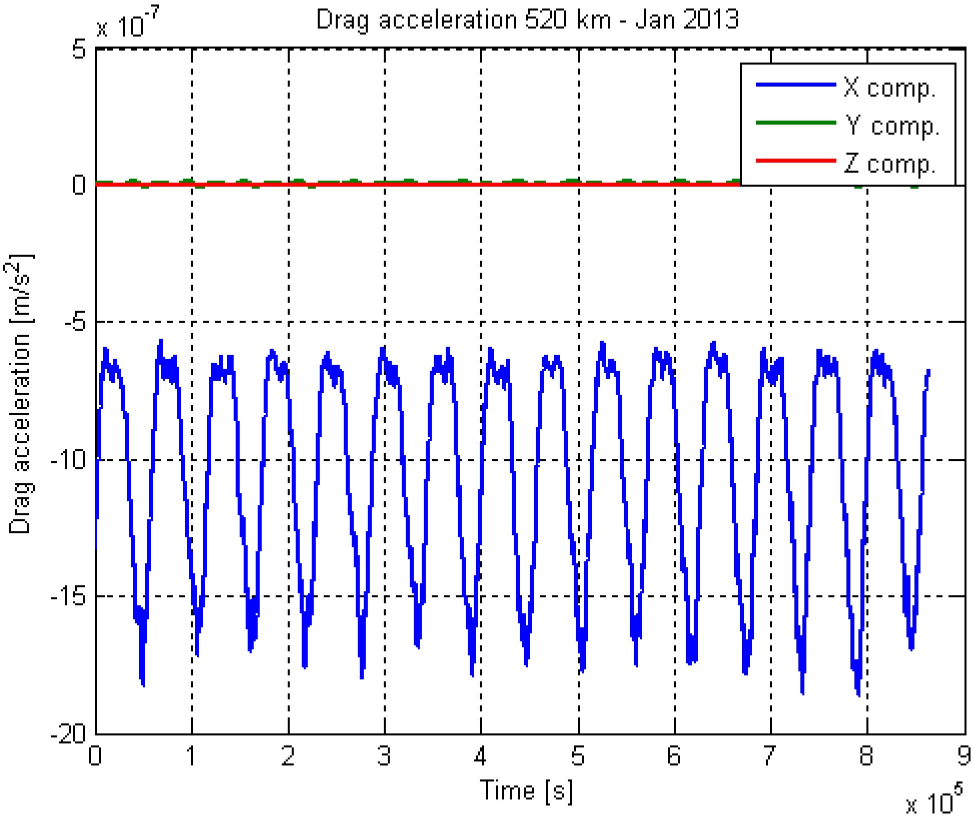

Figure 5.3-2: Drag acceleration at 520 km - Year 2013

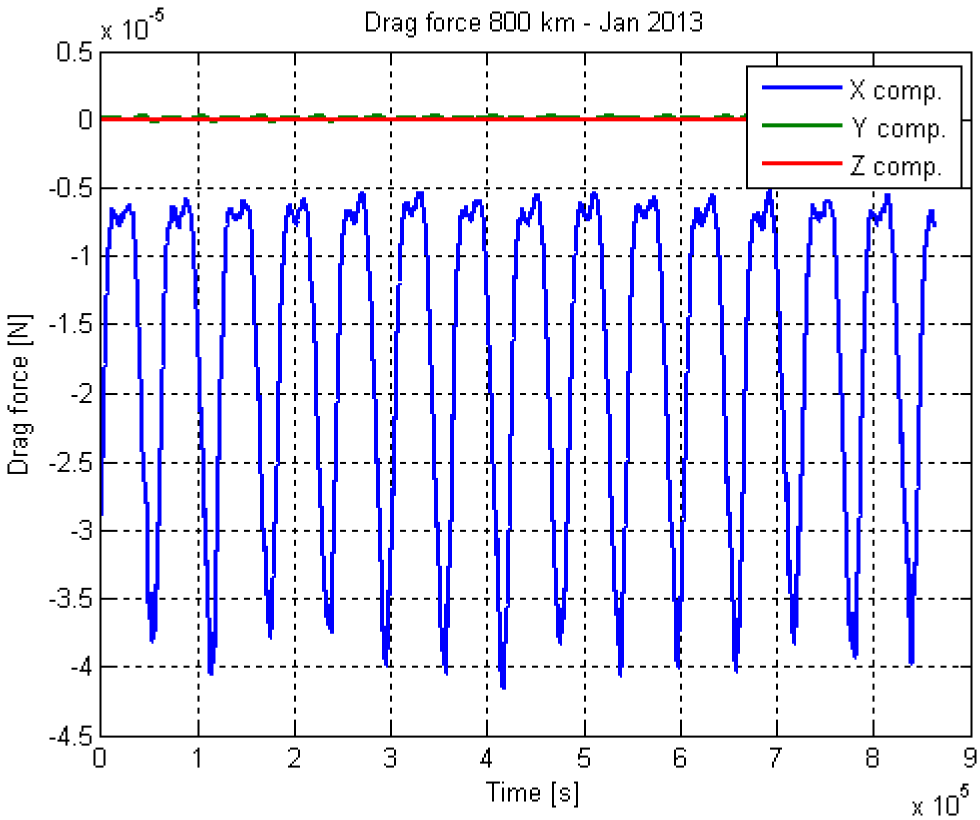

Figure 5.3-3: Drag force at 800 km - Year 2013

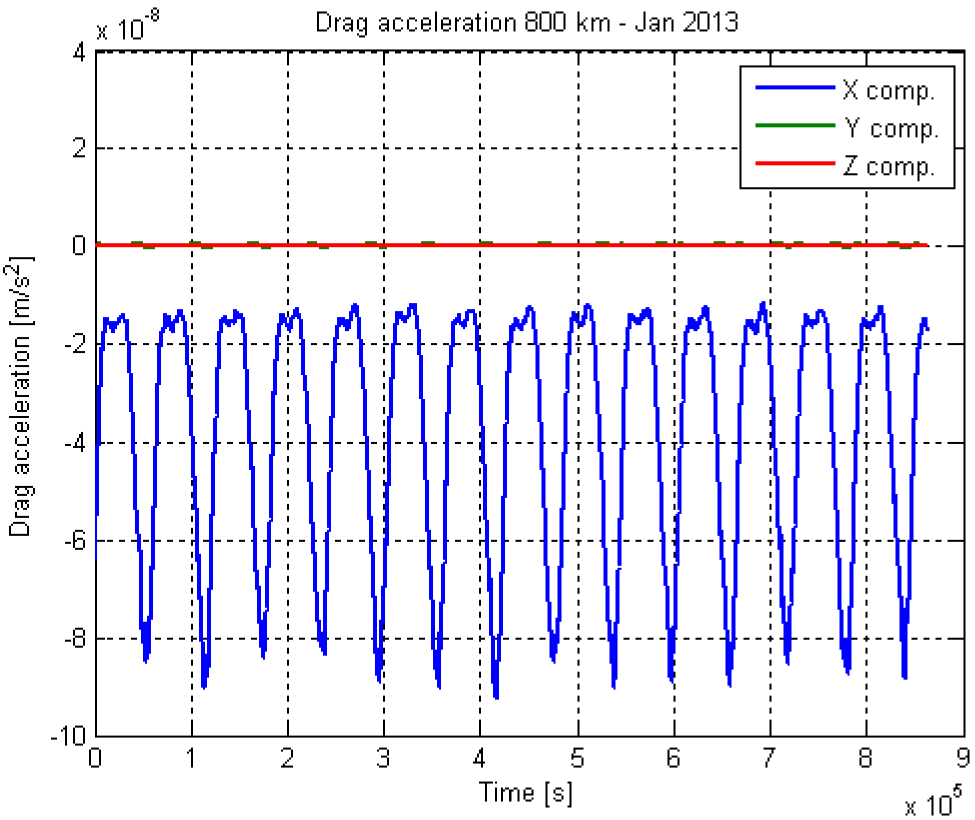

Figure 5.3-4: Drag acceleration at 800 km - Year 2013

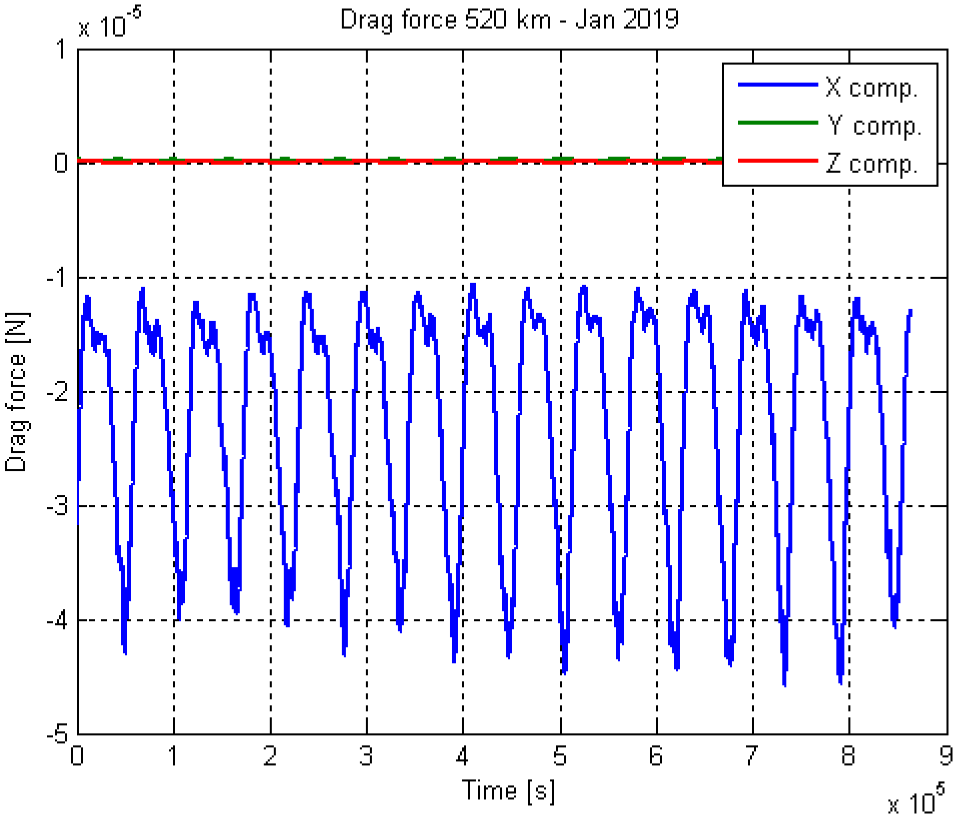

Figure 5.3-5: Drag force at 520 km - Year 2019

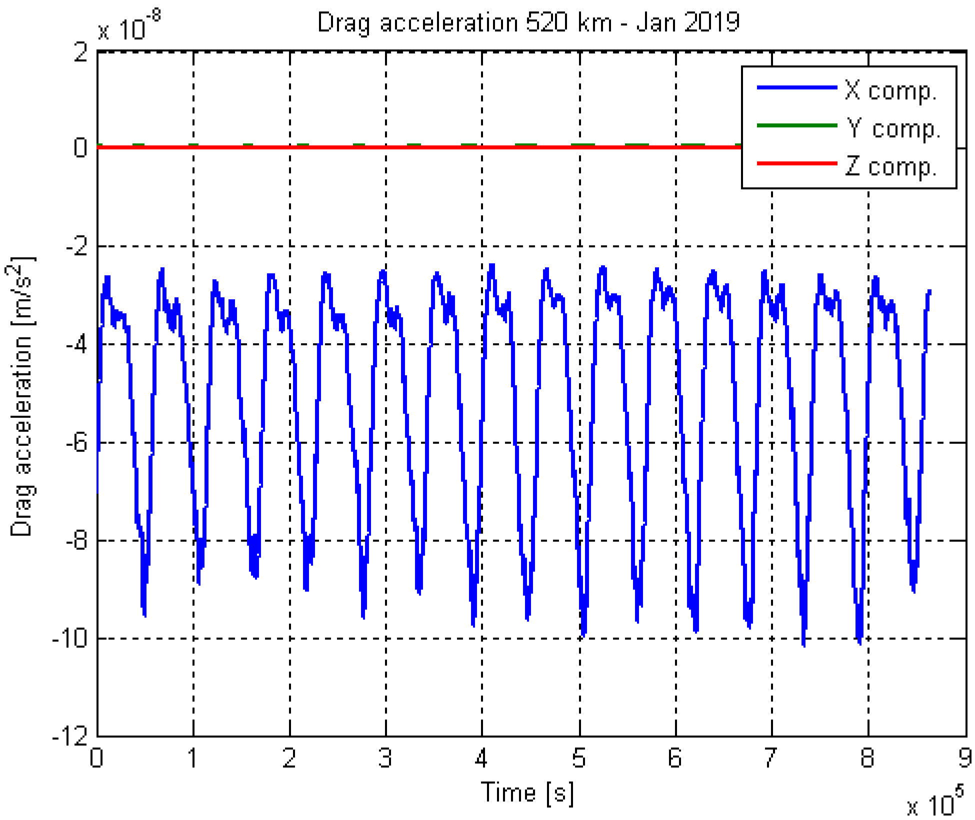

Figure 5.3-6: Drag acceleration at 520 km - Year 2019

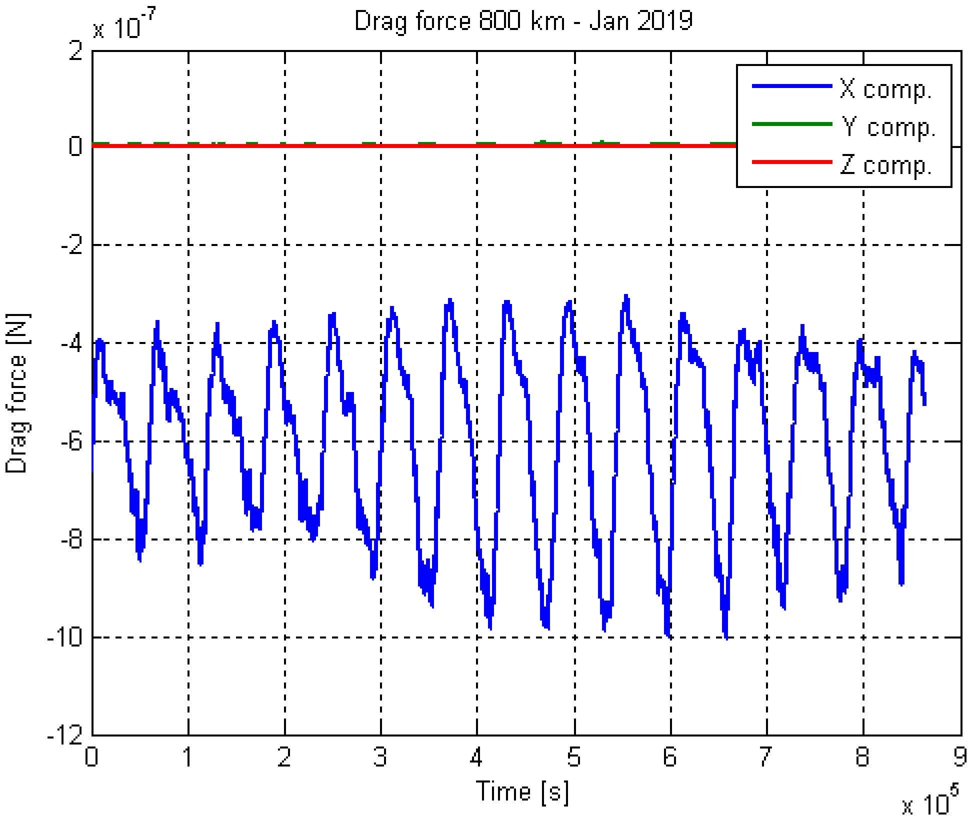

Figure 5.3-7: Drag force at 800 km - Year 2019

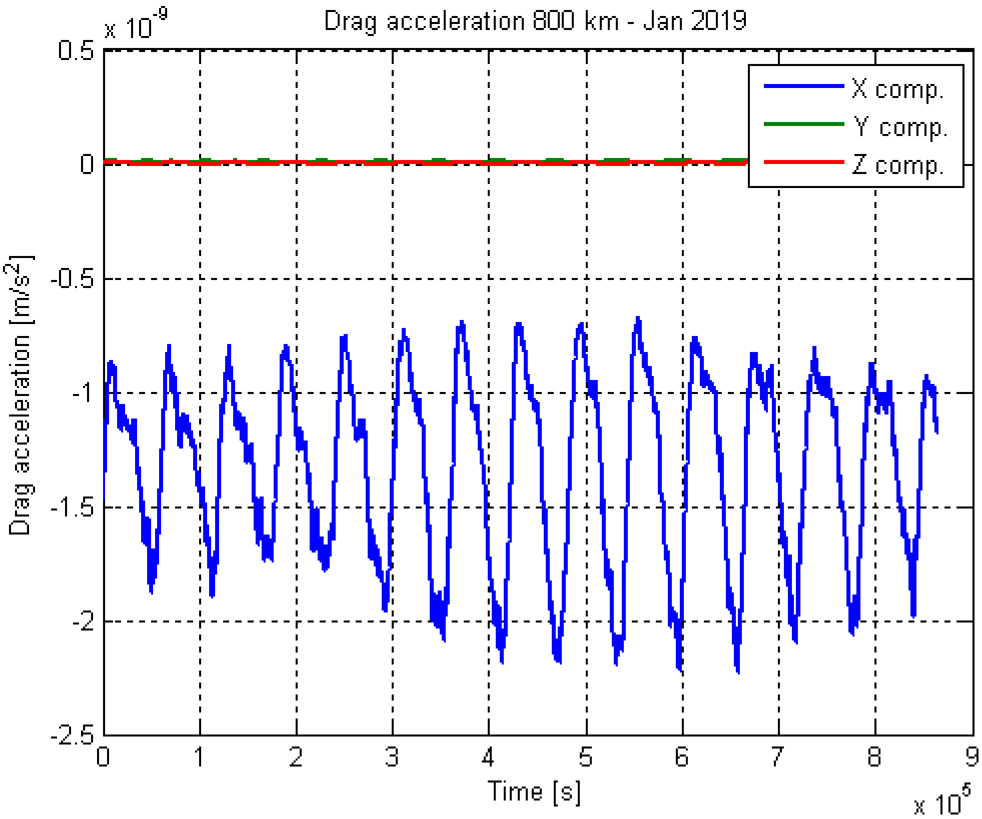

Figure 5.3-8: Drag acceleration at 800 km - Year 2019

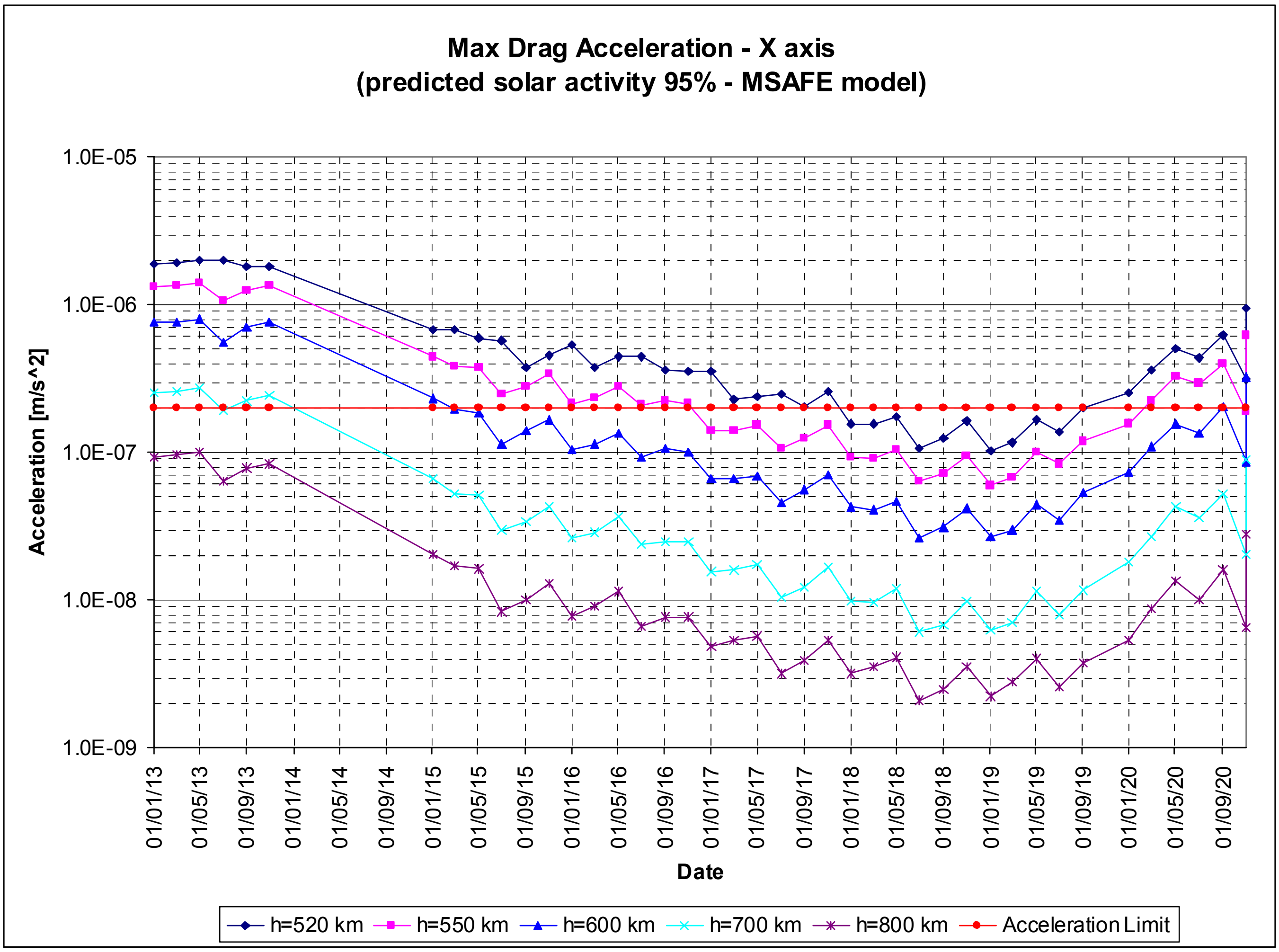

Figure 5.3-9: Parametric analysis of the drag acceleration.

The atmospheric density is taken at the 95% probability level according to the NASA forecast of June 2008. The area-to-mass ratio is 0.0046 m²/kg. A maximum drag acceleration level < 2.0E-7 m/s² first becomes available at mean orbit altitude < 600 km in January 2015.

5.4 Solar Radiation Pressure

Figure 5.4-1 and Figure 5.4-2 show the value of the radiation pressure force, for a number of orbits, at epoch 2013 and 2019. The maximum acceleration is < 4×10^{-8} m/s^2, i.e. < 20% of the acceleration threshold assumed, almost independent of epoch.

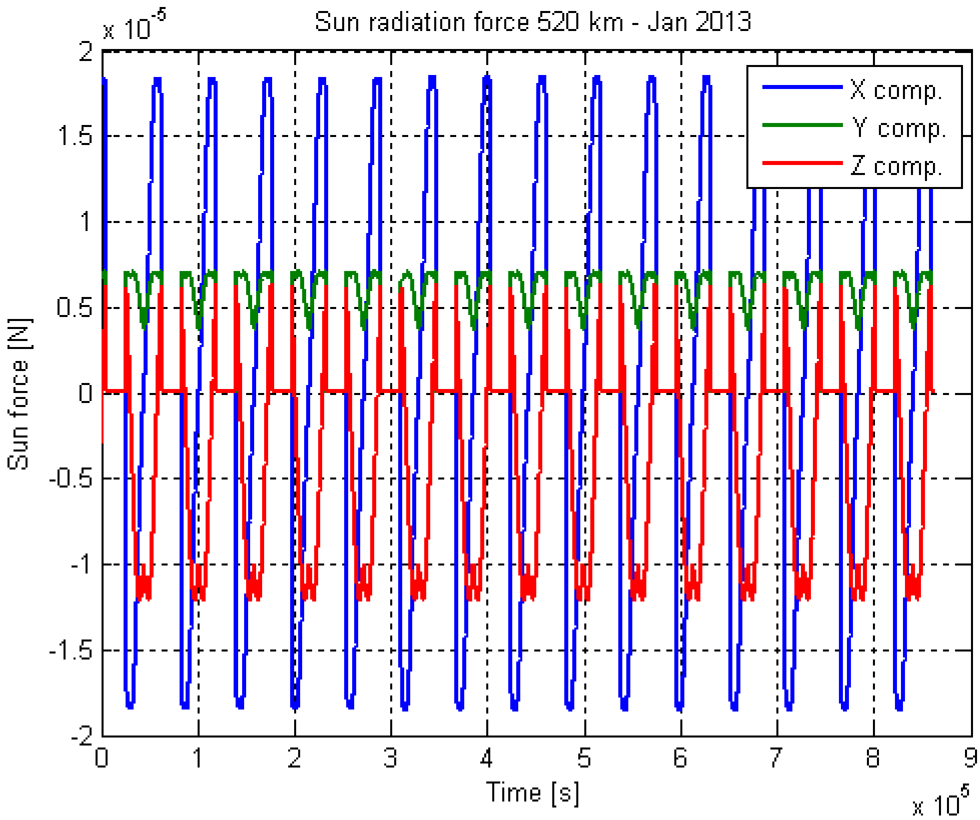

Figure 5.4-1: Solar Radiation Pressure force – Year 2013

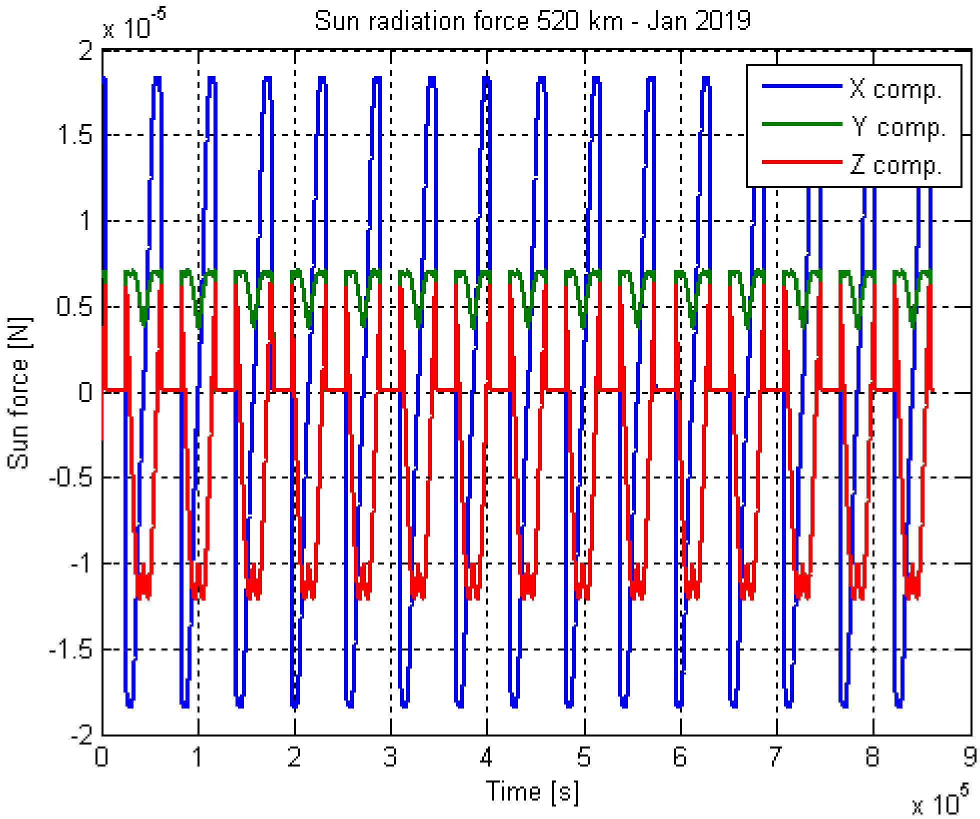

Figure 5.4-2: Solar Radiation Pressure force – Year 2019

5.5 Power Spectral Density of the Disturbing Forces

Figure 5.5-1 and Figure 5.5-2 show examples of the PSD analysis of the drag forces, for an orbit height of 520 km and years 2015 and 2018.

The analysis parameters are:

Parameter	Units	Value
Sampling frequency	Hz	0.1
Npsd	-	12
Nfft (number of FFT points used to calculate the PSD)	-	2^{npsd}
Window	-	Hanning

Table 5.5-1: PSD parameters

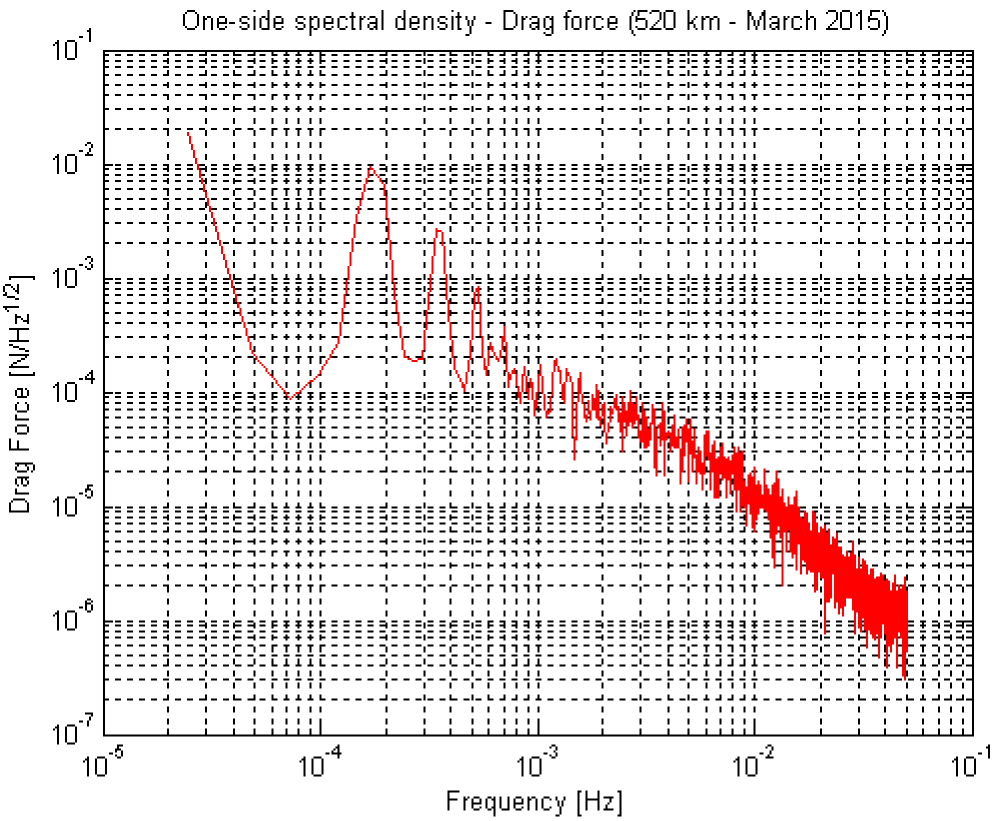

Figure 5.5-1: Square root of the PSD of the drag forces [N Hz$^{-½}$]

520 km altitude – Epoch 2015

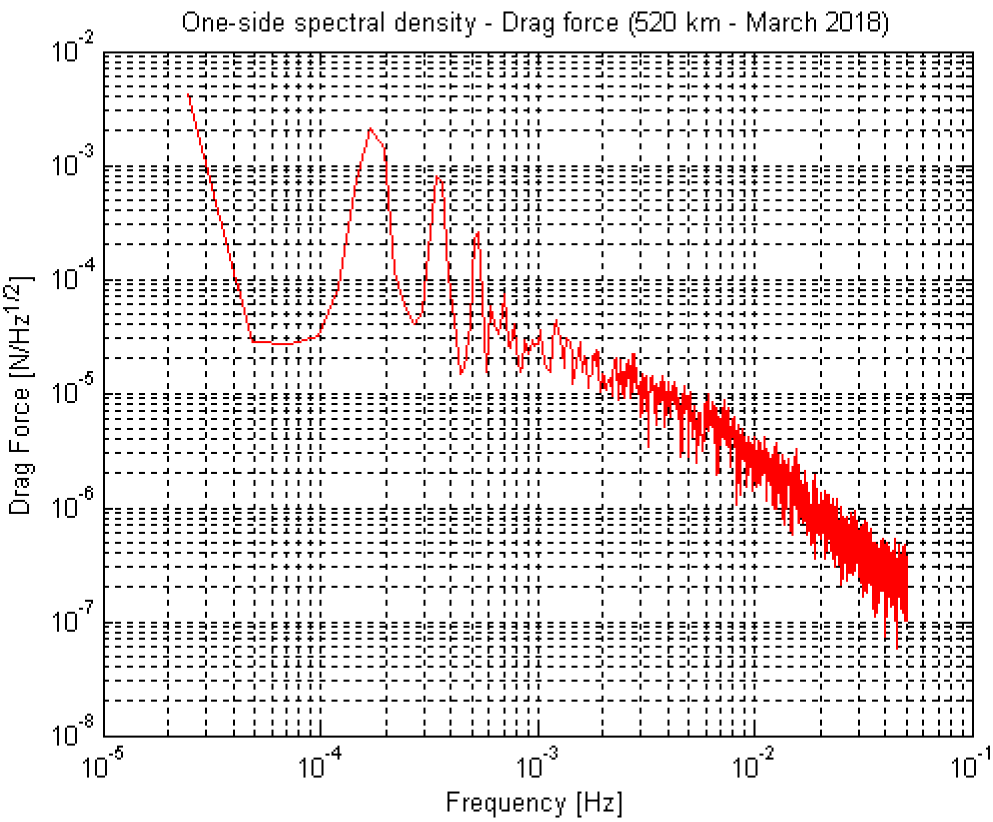

Figure 5.5-2: Square root of the PSD of the drag forces [N Hz$^{-½}$]

520 km altitude – Epoch 2018

Figure 5.5-3 and Figure 5.5-4 show examples of the PSD analysis of the sum of drag and sun forces for an orbit height of 520 km and years 2015 and 2018. The PSD parameters are the same as for the previous figures. The resulted sum forces are represented respectively for 2015 and 2018 in Figure 5.5-5 and Figure 5.5-6.

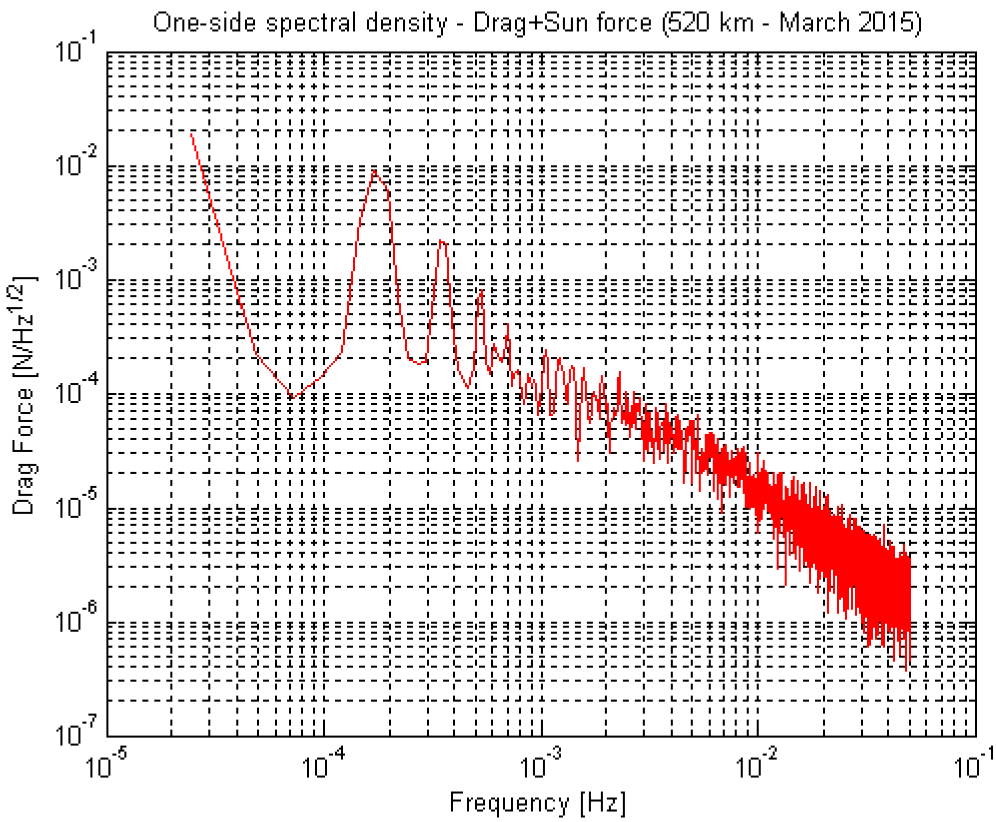

Figure 5.5-3: Square root of the PSD of the disturbing (Drag + Sun) forces [N Hz$^{-½}$]

520 km altitude – Epoch 2015

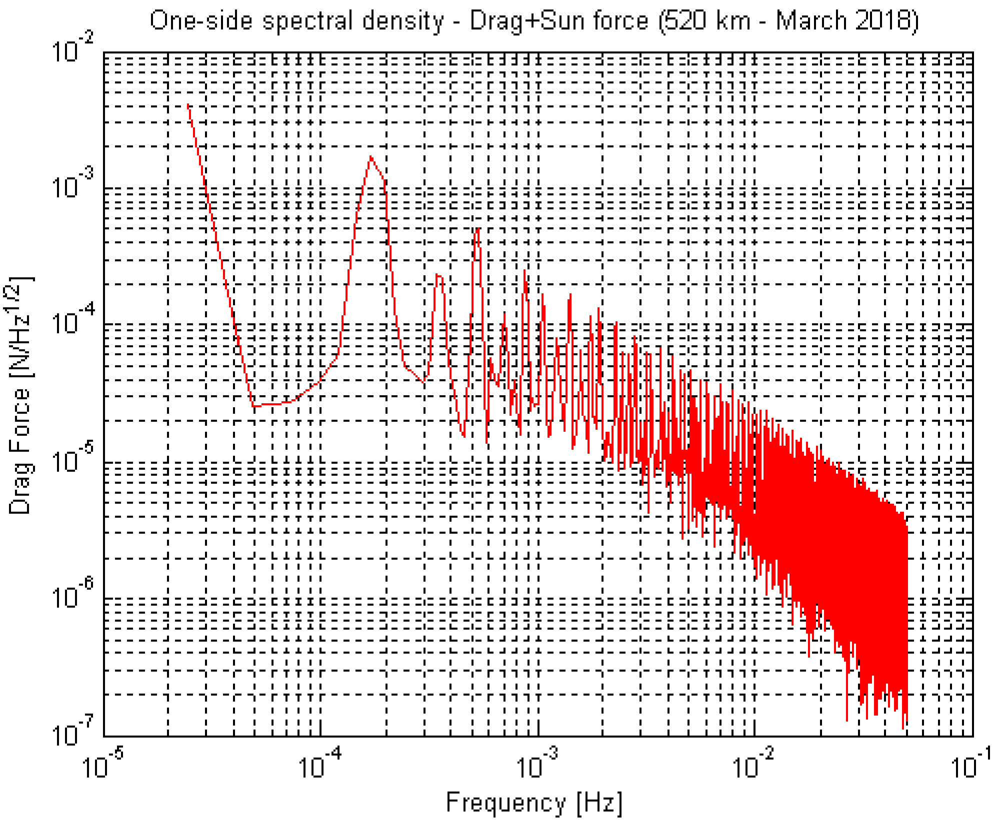

Figure 5.5-4: Square root of the PSD of the disturbing (Drag + Sun) forces [N Hz$^{-½}$]
520 km altitude – Epoch 2018

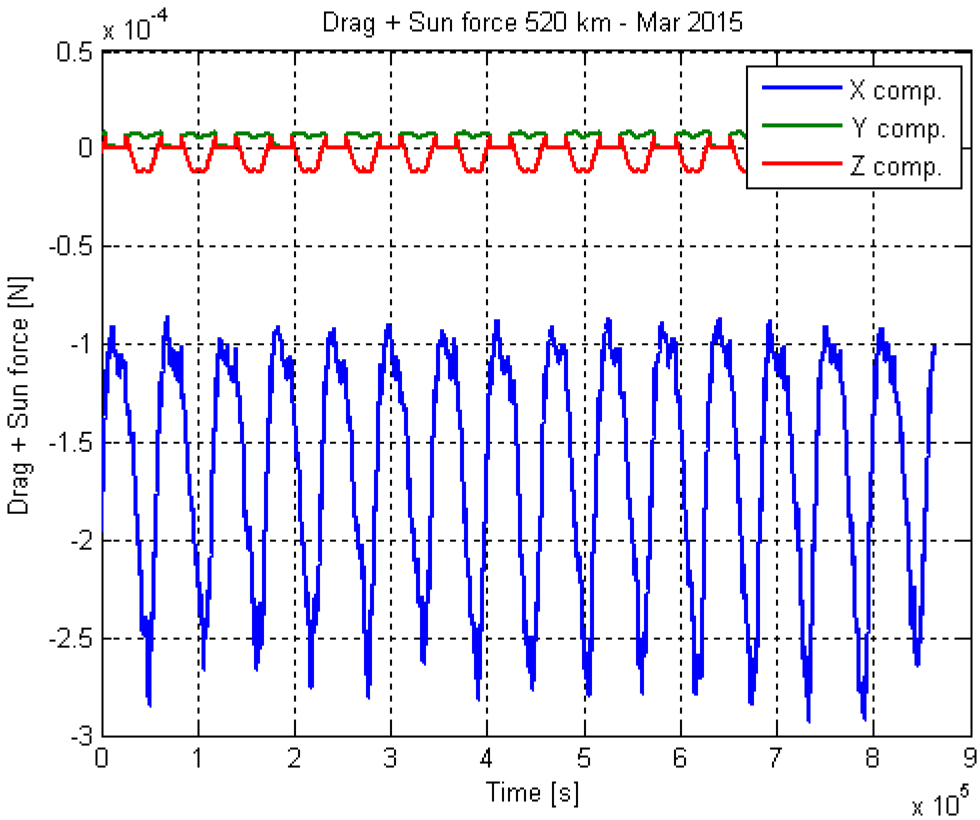

Figure 5.5-5: Drag + Sun forces – 520 km, March 2015

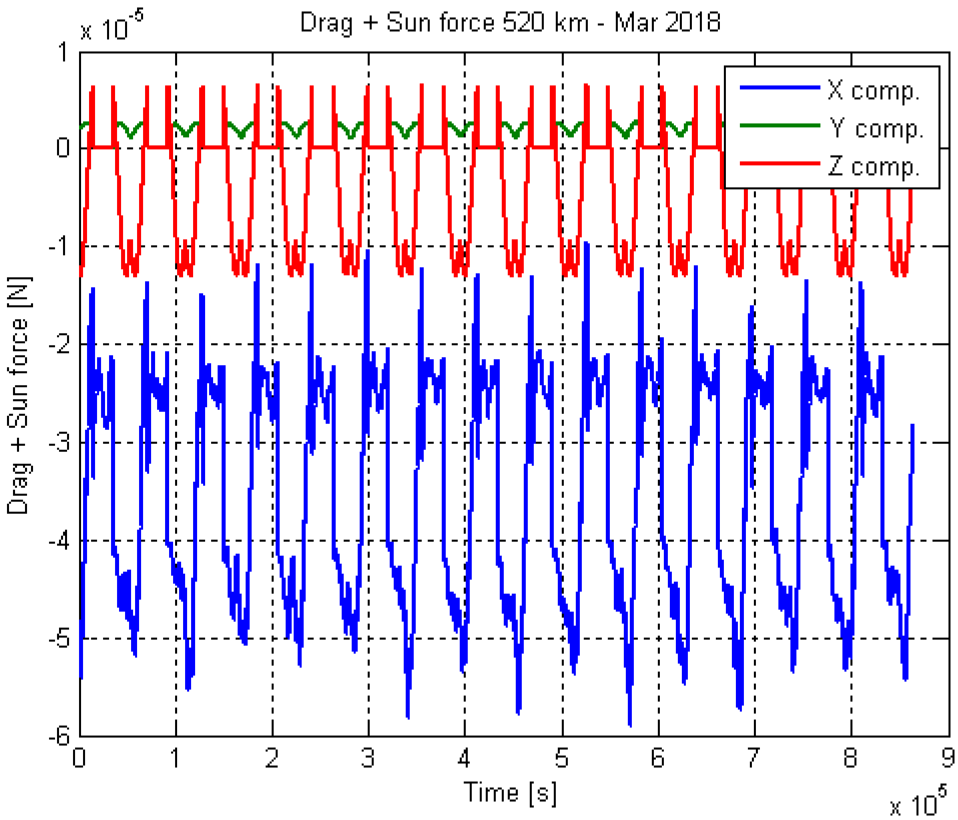

Figure 5.5-6: Drag + Sun forces – 520 km, March 2018

6. MAGNETIC FIELD ANALYSIS

Both the intensity of the Earth's magnetic field and the angle between the magnetic field vector and the orbit normal vector have been calculated using the STK tool.

The next figures show the angle between the magnetic field vector and the orbit normal vector for the baseline equatorial orbit of 520 km, respectively for one orbit and one day period.

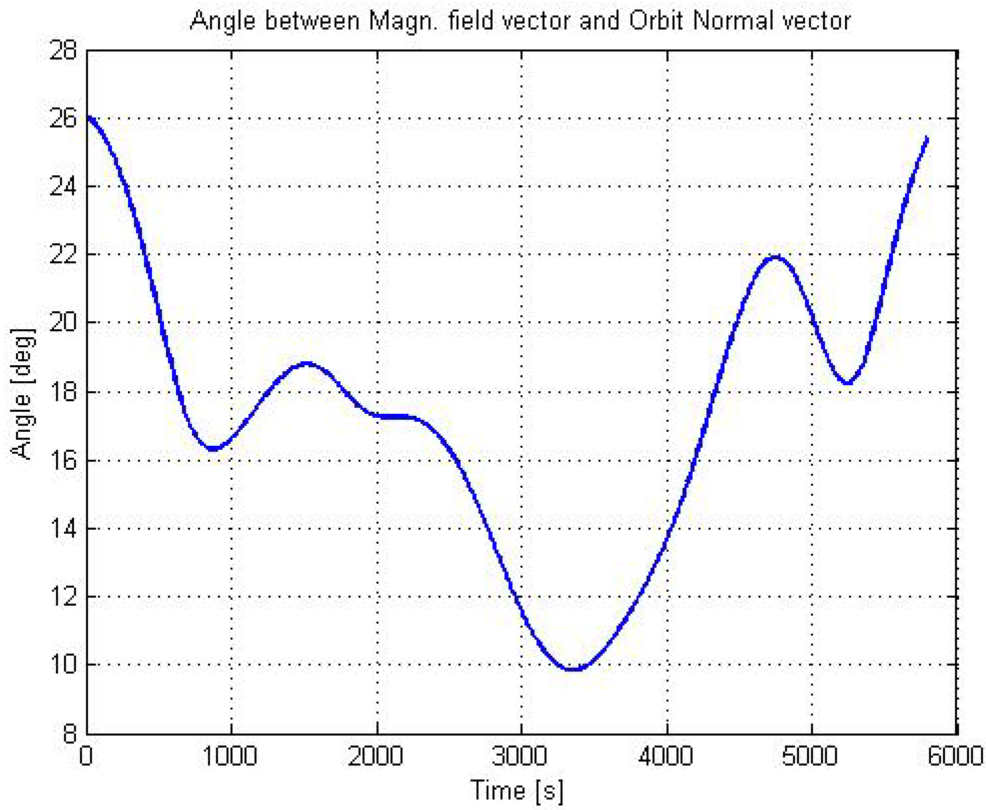

Figure 5.5-1: Angle btw. Magnetic field and Orbit normal (one orbit)

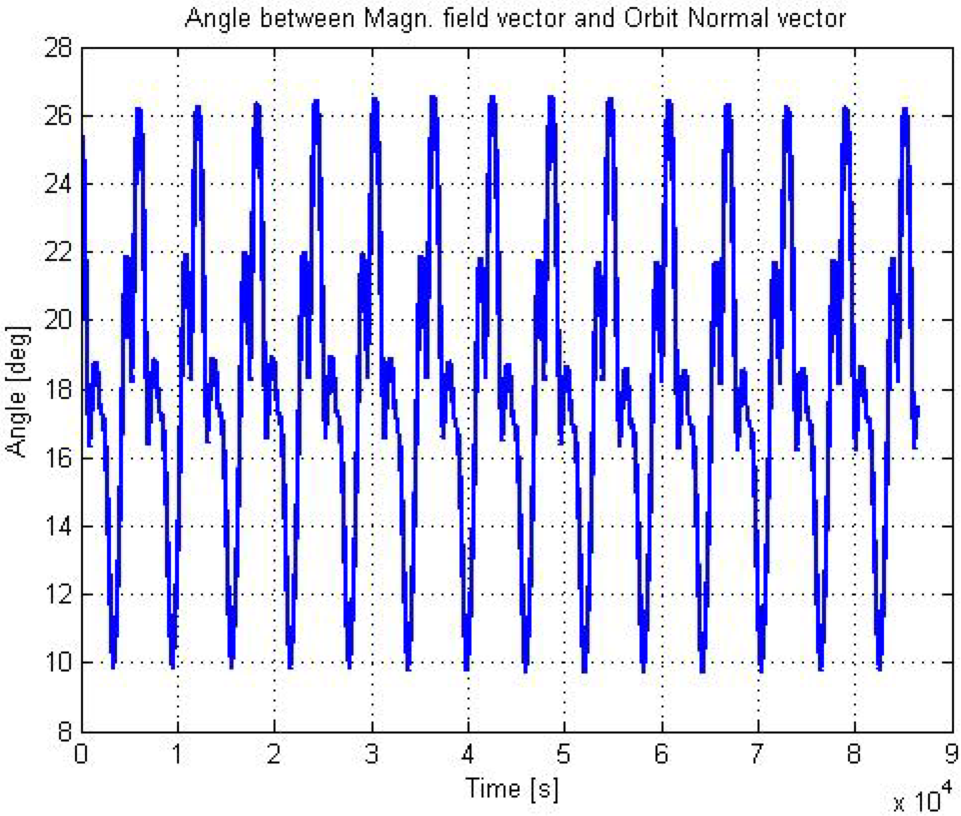

Figure 5.5-2: Angle btw. Magnetic field and Orbit normal (one day)

Magnetic field intensity is represented in graphs below, respectively for one orbit and one day period. Figure 5.5-5 to Figure 5.5-7 show the magnetic field vector components in an Earth inertial reference frame for one day simulation.

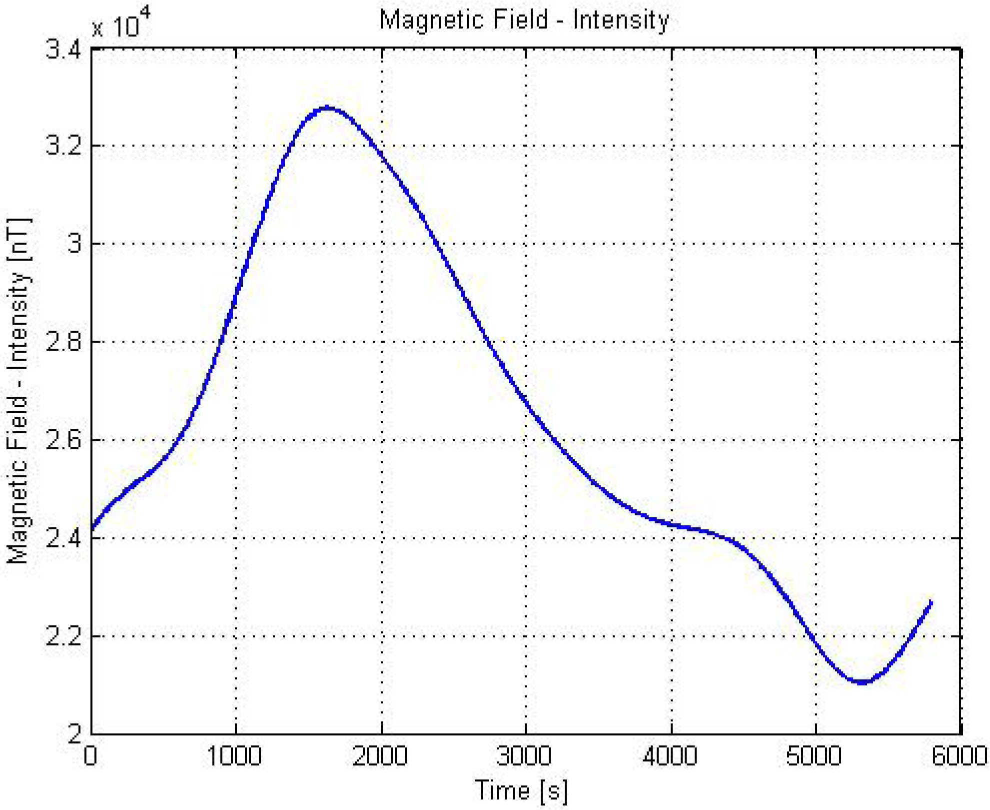

Figure 5.5-3: Magnetic field intensity (one orbit)

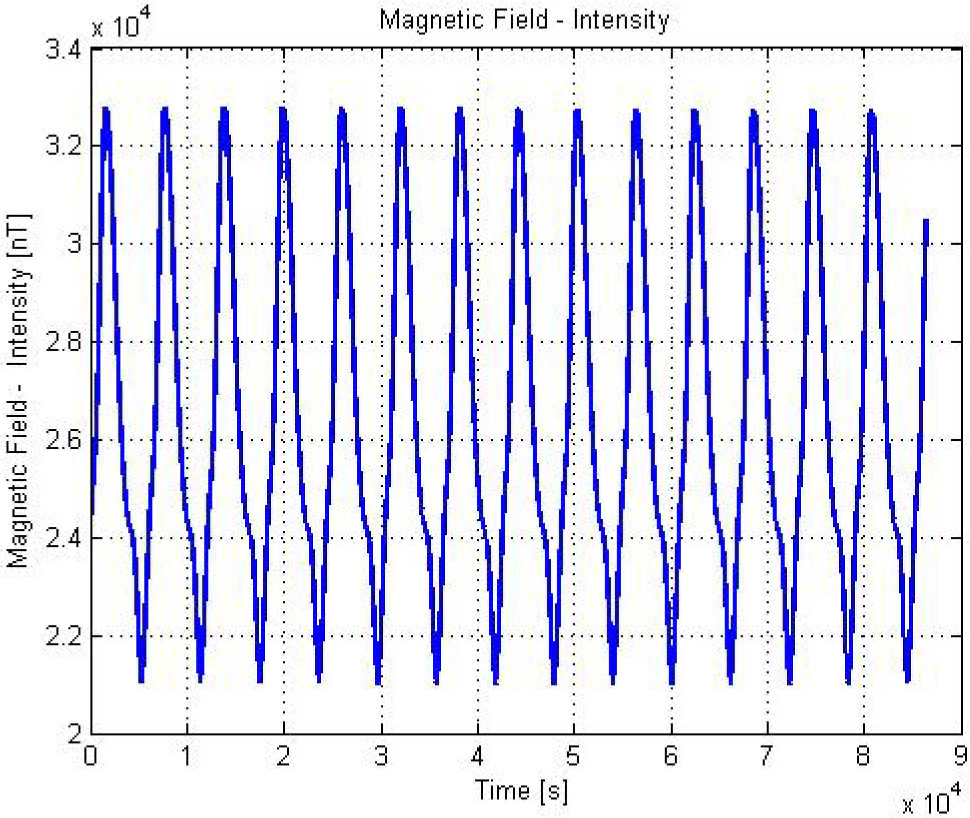

Figure 5.5-4: Magnetic field intensity (one day)

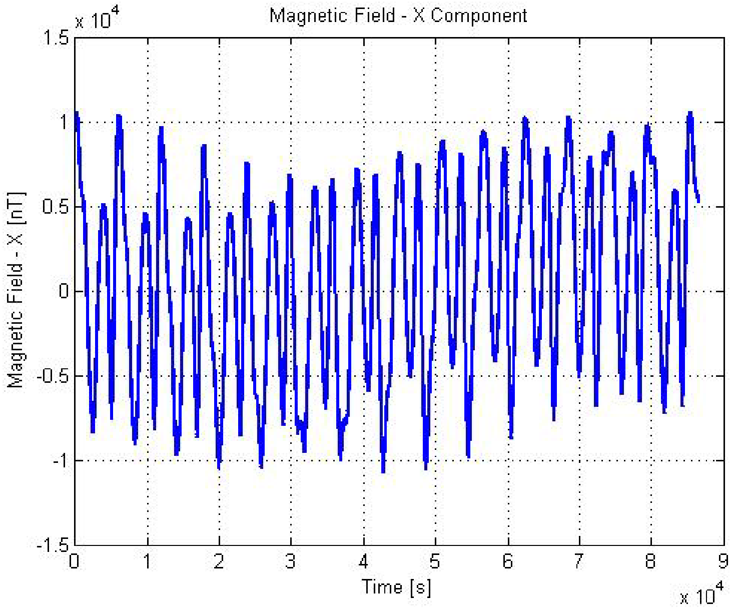

Figure 5.5-5: Magnetic field X component (one day)

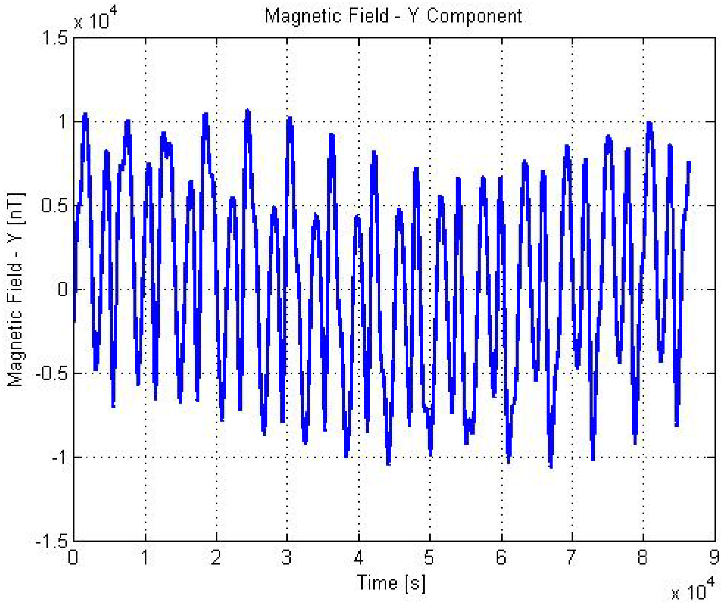

Figure 5.5-6: Magnetic field Y component (one day)

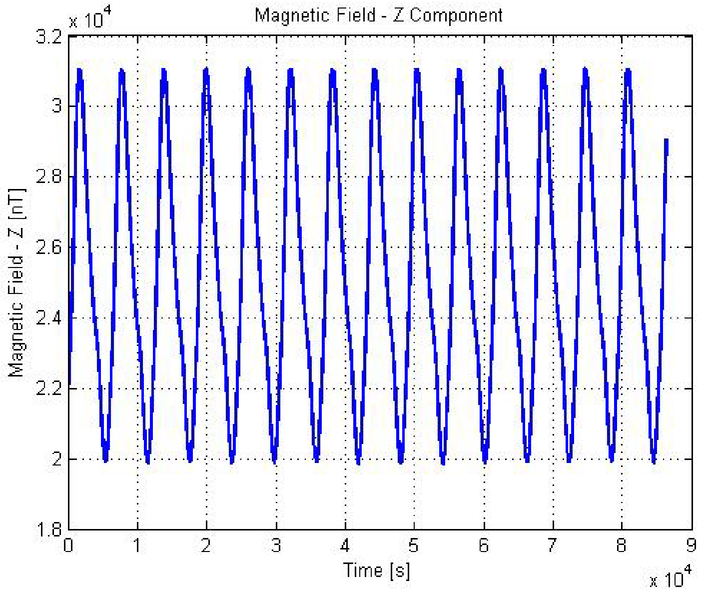

Figure 5.5-7: Magnetic field Z component (one day)

END OF DOCUMENT